Electronic Supplementary Material (ESI) for Energy Advances.
This journal is © The Royal Society of Chemistry 2023

Structure and Interactions of Novel Ether-functionalised Morpholinium and Piperidinium Ionic Liquids with Lithium Salts

Anna Warrington,[a,c] Luke A. O'Dell,[b] Oliver E. Hutt,[c] Maria Forsyth[a] and Jennifer M. Pringle[a]*

[a] Institute for Frontier Materials, Deakin University, Burwood, VIC 3125, Australia

[b] Institute for Frontier Materials, Deakin University, Geelong, VIC 3216, Australia

[c] Boron Molecular, 500 Princes Hwy, Noble Park, VIC 3174, Australia

*Email: jenny.pringle@deakin.edu.au

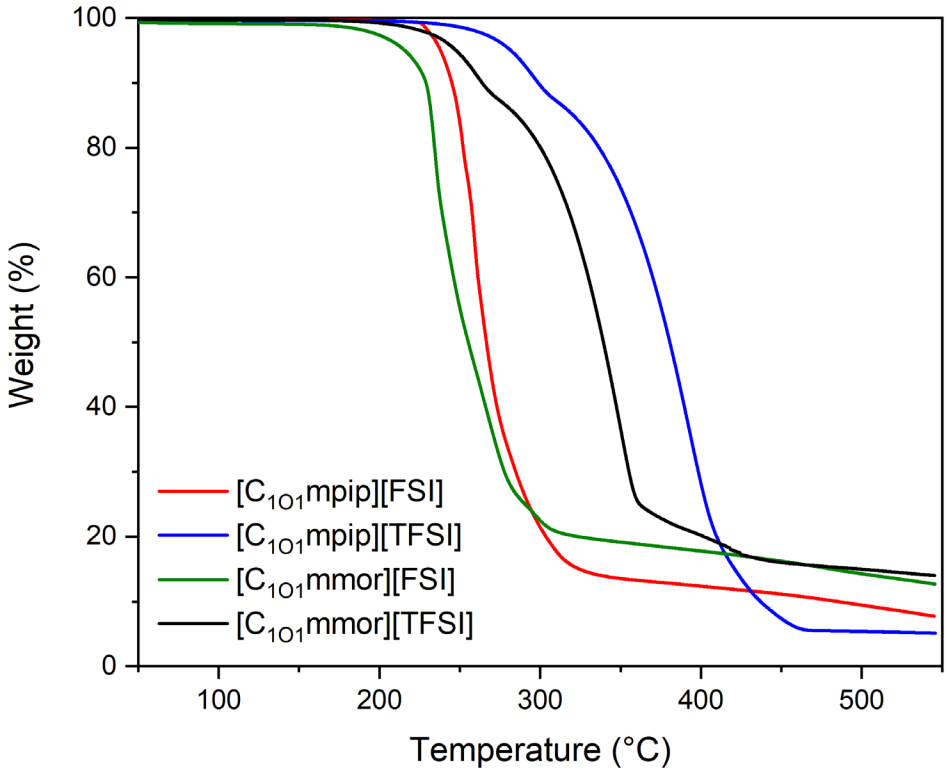

Figure S1. Thermogravimetric analysis of the neat ILs.

Table S1. Density values (g cm^{-1}) of neat ionic liquids and their electrolyte solutions in the temperature range 25-90 °C.

	Density, ρ (g cm^{-1})							
Sample	**25 °C**	**30 °C**	**40 °C**	**50 °C**	**60 °C**	**70 °C**	**80 °C**	**90 °C**
$[C_{1O1}mpip][FSI]$	1.38	1.383	1.375	1.367	1.359	1.350	1.342	1.334
$(LiFSI)_{0.1}([C_{1O1}mpip][FSI])_{0.9}$	1.410	1.406	1.397	1.389	1.380	1.372	1.364	1.356
$[C_{1O1}mmor][FSI]$	1.472	1.467	1.458	1.450	1.441	1.433	1.425	1.416
$(LiFSI)_{0.1}([C_{1O1}mmor][FSI])_{0.9}$	1.494	1.489	1.480	1.471	1.463	1.454	1.446	1.437
$[C_{1O1}mpip][TFSI]$	1.468	1.463	1.454	1.444	1.435	1.426	1.417	1.408
$(LiTFSI)_{0.1}([C_{1O1}mpip][TFSI])_{0.9}$	1.489	1.485	1.475	1.465	1.456	1.446	1.437	1.428
$[C_{1O1}mmor][TFSI]$	1.541	1.536	1.526	1.517	1.507	1.498	1.489	1.479
$(LiTFSI)_{0.1}([C_{1O1}mmor][TFSI])_{0.9}$	1.557	1.552	1.542	1.532	1.522	1.513	1.503	1.494

The density data from Table S1 was fit to Equation S1 and all have correlation coefficients greater than 0.999, verifying a linear temperature dependence.

$$\rho = a + bT \tag{S1}$$

Where ρ is the density (g cm^{-3}), T is the temperature (K) and *a* and *b* are linear fitting parameters that represent extrapolated density at 0 K and the coefficient of volume expansion (g cm^{-3} K^{-1}), respectively. The parameters for Eq. S1 are summarised in Table S2.

Table S2. Linear fit parameters for temperature-dependant density of neat ionic liquids and their electrolyte solutions. All R^2 values are above 0.9999.

Sample	*a* (g cm^{-3})	10^4 *b* (g cm^{-3} K^{-1})
$[C_{1O1}mpip][FSI]$	1.63	-8.19
$(LiFSI)_{0.1}([C_{1O1}mpip][FSI])_{0.9}$	1.66	-8.33
$[C_{1O1}mmor][FSI]$	1.72	-8.50
$(LiFSI)_{0.1}([C_{1O1}mmor][FSI])_{0.9}$	1.75	-8.70
$[C_{1O1}mpip][TFSI]$	1.74	-9.27
$(LiTFSI)_{0.1}([C_{1O1}mpip][TFSI])_{0.9}$	1.77	-9.51
$[C_{1O1}mmor][TFSI]$	1.82	-9.50
$(LiTFSI)_{0.1}([C_{1O1}mmor][TFSI])_{0.9}$	1.84	-9.66

Table S3. Viscosity values (mPa s) of neat ionic liquids and their electrolyte solutions in the temperature range 25-90 °C.

	Viscosity (mPa s)							
Sample	**25 °C**	**30 °C**	**40 °C**	**50 °C**	**60 °C**	**70 °C**	**80 °C**	**90 °C**
$[C_{1O1}mpip][FSI]$	60.8	51.8	35.7	25.7	20.8	16.4	13.2	10.9
$(LiFSI)_{0.1}([C_{1O1}mpip][FSI])_{0.9}$	68.7	56.1	40.3	29.2	22.0	17.3	14.0	11.5
$[C_{1O1}mmor][FSI]$	138.8	105.9	67.1	47.8	33.1	24.0	18.8	15.6
$(LiFSI)_{0.1}([C_{1O1}mmor][FSI])_{0.9}$	188.6	143.6	87.4	57.5	40.0	29.3	22.2	16.4
$[C_{1O1}mpip][TFSI]$	90.6	71.5	46.5	32.4	23.6	17.9	13.9	11.2
$(LiTFSI)_{0.1}([C_{1O1}mpip][TFSI])_{0.9}$	141.7	108.0	66.9	46.5	30.1	21.9	16.6	13.1
$[C_{1O1}mmor][TFSI]$	273.4	198.0	111.9	68.9	45.8	32.0	23.3	17.7
$(LiTFSI)_{0.1}([C_{1O1}mmor][TFSI])_{0.9}$	407.1	290.2	154.5	90.5	58.5	41.5	29.5	22.1

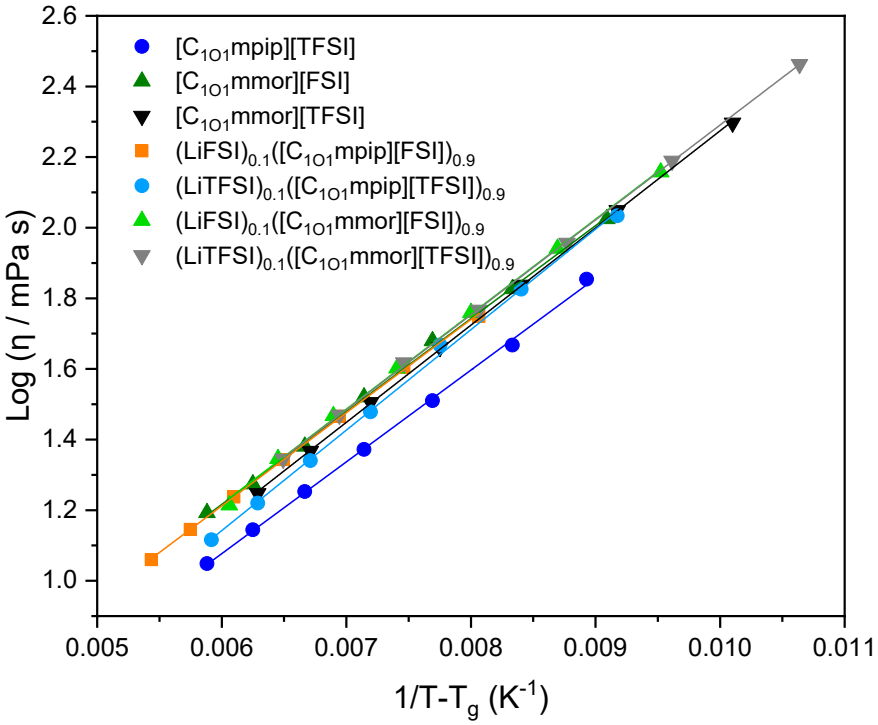

Figure S2. VTF plot of viscosities for ionic liquids and their electrolytes. $[C_{1O1}mpip][FSI]$ is excluded as there was no Tg present in the DSC graph within the temperature range recorded.

Table S4. Conductivity values (mS cm^{-1}) of neat ionic liquids and their electrolyte solutions in the temperature range 30-90 °C.

	Conductivity (mS cm^{-1})						
Sample	**30 °C**	**40 °C**	**50 °C**	**60 °C**	**70 °C**	**80 °C**	**90 °C**
$[C_{1O1}mpip][FSI]$	5.9	7.9	10.4	13.2	16.2	19.6	23.2
$(LiFSI)_{0.1}([C_{1O1}mpip][FSI])_{0.9}$	5.0	6.9	9.1	11.6	14.4	17.5	20.8
$[C_{1O1}mmor][FSI]$	2.9	4.3	6.0	8.0	10.4	13.1	16.0
$(LiFSI)_{0.1}([C_{1O1}mmor][FSI])_{0.9}$	2.2	3.3	4.7	6.2	8.0	10.0	12.0
$[C_{1O1}mpip][TFSI]$	3.0	4.5	6.2	8.2	10.5	13.1	15.9
$(LiTFSI)_{0.1}([C_{1O1}mpip][TFSI])_{0.9}$	2.0	3.0	4.4	6.0	7.9	10.0	12.4
$[C_{1O1}mmor][TFSI]$	1.2	2.1	3.3	4.7	6.5	8.4	10.6
$(LiTFSI)_{0.1}([C_{1O1}mmor][TFSI])_{0.9}$	0.8	1.4	2.2	3.3	4.6	6.2	8.0

Table S5. Fitting parameters for the conductivity (σ) using the Vogel-Tammann-Fulcher equation of the ionic liquids.

Ionic liquid	σ_0 / mS cm^{-1}	$\Delta\sigma_0$ / mS cm^{-1}	B_σ /K	ΔB_σ /K	$T_{0,\sigma}$ /K	$\Delta T_{0,\sigma}$ /K	R^2
$[C_{1O1}mpip][FSI]$	581	10	647	13	162	1.6	0.99999
$(LiFSI)_{0.1}([C_{1O1}mpip][FSI])_{0.9}$	478	11	602	21	171	2.7	0.99998
$[C_{1O1}mmor][FSI]$	509	11	623	14	183	1.7	0.99999
$(LiFSI)_{0.1}([C_{1O1}mmor][FSI])_{0.9}$	223	12	482	36	205	4.5	0.99989
$[C_{1O1}mpip][TFSI]$	336	11	520	34	193	4.3	0.99993
$(LiTFSI)_{0.1}([C_{1O1}mpip][TFSI])_{0.9}$	427	12	625	48	205	5.1	0.99989
$[C_{1O1}mmor][TFSI]$	274	11	493	26	212	2.9	0.99994
$(LiTFSI)_{0.1}([C_{1O1}mmor][TFSI])_{0.9}$	495	11	689	33	196	3.1	0.99996

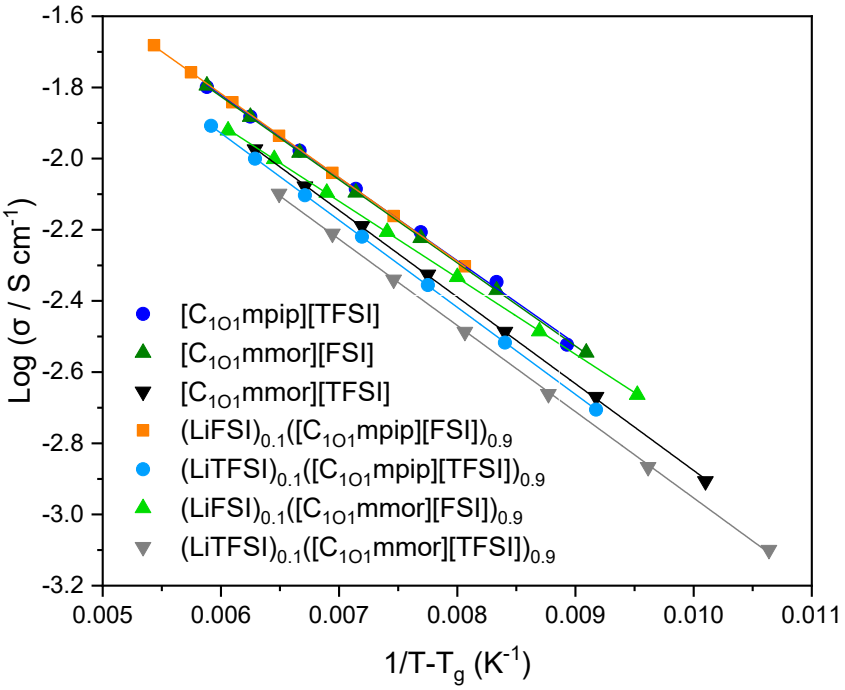

Figure S3. VTF plot of conductivities for ionic liquids and their electrolytes. $[C_{1O1}mpip][FSI]$ is excluded as there was no Tg present in the DSC graph within the temperature range recorded.

Table S6. ΔW of neat ionic liquids and their electrolyte solutions in the temperature range 30-90 °C.

	ΔW						
Sample	**30 °C**	**40 °C**	**50 °C**	**60 °C**	**70 °C**	**80 °C**	**90 °C**
$[C_{1O1}mpip][FSI]$	0.15	0.17	0.20	0.18	0.20	0.20	0.21
$(LiFSI)_{0.1}([C_{1O1}mpip][FSI])_{0.9}$	0.21	0.21	0.22	0.24	0.25	0.25	0.26
$[C_{1O1}mmor][FSI]$	0.17	0.19	0.19	0.22	0.25	0.25	0.24
$(LiFSI)_{0.1}([C_{1O1}mmor][FSI])_{0.9}$	0.19	0.22	0.25	0.27	0.30	0.32	0.37
$[C_{1O1}mpip][TFSI]$	0.21	0.21	0.23	0.24	0.25	0.26	0.27
$(LiTFSI)_{0.1}([C_{1O1}mpip][TFSI])_{0.9}$	0.23	0.25	0.24	0.29	0.31	0.32	0.33
$[C_{1O1}mmor][TFSI]$	0.17	0.17	0.20	0.21	0.23	0.25	0.27
$(LiTFSI)_{0.1}([C_{1O1}mmor][TFSI])_{0.9}$	0.21	0.25	0.27	0.29	0.29	0.30	0.31

Table S7. Molar conductivity values (S cm^2 mol^{-1}) calculated from specific conductivity and density of neat ionic liquids and their electrolyte solutions in the temperature range 30-90 °C.

	Molar Conductivity by EIS (S cm^2 mol^{-1})						
Sample	**30 °C**	**40 °C**	**50 °C**	**60 °C**	**70 °C**	**80 °C**	**90 °C**
$[C_{1O1}mpip][FSI]$	1.4	1.9	2.5	3.	3.9	4.7	5.6
$(LiFSI)_{0.1}([C_{1O1}mpip][FSI])_{0.9}$	1.1	1.5	2.0	2.6	3.3	4.0	4.8
$[C_{1O1}mmor][FSI]$	0.6	1.0	1.4	1.8	2.4	3.0	3.7
$(LiFSI)_{0.1}([C_{1O1}mmor][FSI])_{0.9}$	0.5	0.7	1.0	1.3	1.7	2.2	2.6
$[C_{1O1}mpip][TFSI]$	0.9	1.3	1.8	2.4	3.1	3.9	4.8
$(LiTFSI)_{0.1}([C_{1O1}mpip][TFSI])_{0.9}$	0.5	0.8	1.2	1.8	2.2	2.9	3.6
$[C_{1O1}mmor][TFSI]$	0.3	0.6	0.9	1.3	1.8	2.4	3.1
$(LiTFSI)_{0.1}([C_{1O1}mmor][TFSI])_{0.9}$	0.2	0.4	0.6	0.9	1.3	1.7	2.2

Table S8. Molar conductivity values (S cm^2 mol^{-1}) calculated from the diffusion coefficients of neat ionic liquids and their electrolyte solutions in the temperature range 30-90 °C.

	Molar Conductivity by PFG-NMR (S cm^2 mol^{-1})					
Sample	**25 °C**	**30 °C**	**40 °C**	**50 °C**	**60 °C**	**70 °C**
$[C_{1O1}mpip][FSI]$	1.4	1.7	2.4	3.2	4.2	5.3
$(LiFSI)_{0.1}([C_{1O1}mpip][FSI])_{0.9}$	1.8	2.1	3.0	4.2	5.6	7.1
$[C_{1O1}mmor][FSI]$	0.7	0.8	1.3	1.8	2.6	3.4
$(LiFSI)_{0.1}([C_{1O1}mmor][FSI])_{0.9}$	0.7	0.9	1.4	2.2	3.3	4.4
$[C_{1O1}mpip][TFSI]$	1.0	1.2	1.8	2.6	3.5	4.6
$(LiTFSI)_{0.1}([C_{1O1}mpip][TFSI])_{0.9}$	0.7	0.9	1.5	2.2	3.1	4.2
$[C_{1O1}mmor][TFSI]$	0.3	0.4	0.7	1.1	1.7	2.5
$(LiTFSI)_{0.1}([C_{1O1}mmor][TFSI])_{0.9}$	0.3	0.4	0.6	1.1	1.7	2.5

The diffusivity ratio of individual ions can be determined from their diffusion coefficients in neat ILs and the electrolytes using the following equation.[1]

$$Diffusivity\ ratio = \frac{x_i D_i}{\Sigma_i x_i D_i}$$

Where x_i is the molar fraction of each individual ion, and D_i is the self-diffusion coefficient of an ion ($m^2\ s^{-1}$). The diffusion coefficients measured by PFG-NMR are averages of all species with a particular nuclei within the system, including individual charged-species, ion-pairs and aggregates. Aggregates diffuse slower than individual species as they have larger radii, which results in lower diffusion coefficients and transport ratios of Li^+. Therefore, the diffusivity ratio of Li^+ calculated via diffusion coefficients typically underestimates the Li-transference calculated by electrochemical techniques.[2,3]

As only 10 mol% LiFSI or LiTFSI was used in each system, the ratio of diffusivity by Li^+ in relation to its molar concentration is low as there is a low number density of lithium ions. In the electrolyte solutions, the diffusivity ratio for Li^+, presented in Table S9, are higher for $[C_{1O1}mmor]^+$ based ionic liquids for both anion types, and the $[FSI]^-$ anion also leads to higher diffusivity ratio for Li^+. $[C_{1O1}mmor][FSI]$ has the highest diffusivity ratio for Li^+ of 0.054. These values, while low, are similar to other systems analysed in this way, such as 0.8 mol kg^{-1} LiFSI (20 mol%) in N-methyl-N-propylpyrrolidinium bis(fluorosulfonyl)imide, $[C_3mpyr][FSI]$, which displayed a diffusivity ratio of 0.08 ± 0.01 at 50 °C,[4] and 23 mol% LiTFSI in N-methyl-N-butylpyrrolidinium bis(trifluoromethanesulfonyl)imide, $[C_4mpyr][TFSI]$, which had a ratio of 0.064, while both of these systems have double the Li^+ concentration.[1]

Table S9. Self-Diffusion coefficients ($m^2\ s^{-1}$) for bulk ionic liquids and electrolyte solutions at 30 °C, and the diffusivity ratio of Li^+ with respect to all the ions in the electrolyte.

Ionic Liquid	$D_s(^1H)$ (10^{-12} $m^2\ s^{-1}$ ± 5%)	$D_s(^{19}F)$ (10^{-12} $m^2\ s^{-1}$ ± 5%)	$D_s(^7Li)$ (10^{-12} $m^2\ s^{-1}$ ± 5%)	Diffusivity ratio of Li^+ with respect to all ions in the electrolyte
$[C_{1O1}mpip][FSI]$	19.6	26.5		
$(LiFSI)_{0.1}([C_{1O1}mpip][FSI])_{0.9}$	18.7	21.2	16.2	0.041 ± 0.002
$[C_{1O1}mmor][FSI]$	8.8	13.0		
$(LiFSI)_{0.1}([C_{1O1}mmor][FSI])_{0.9}$	7.4	9.7	9.3	0.054 ± 0.004
$[C_{1O1}mpip][TFSI]$	18.0	14.2		
$(LiTFSI)_{0.1}([C_{1O1}mpip][TFSI])_{0.9}$	11.7	8.1	5.1	0.027 ± 0.001
$[C_{1O1}mmor][TFSI]$	5.7	5.3		
$(LiTFSI)_{0.1}([C_{1O1}mmor][TFSI])_{0.9}$	3.7	3.2	2.5	0.036 ± 0.001

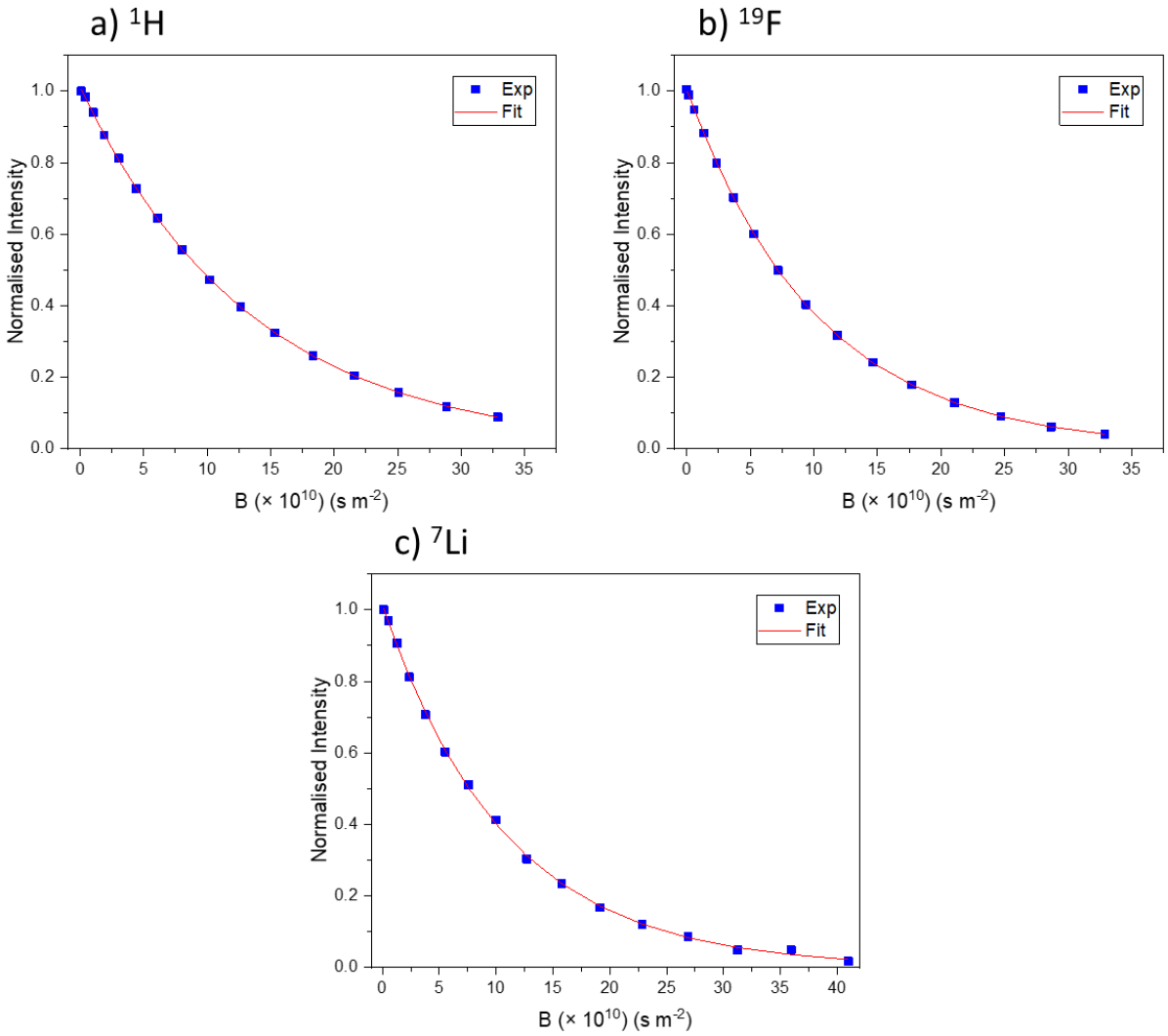

Figure S4. PFG NMR attenuation plots for $(LiFSI)_{0.1}([C_{1O1}mmor][FSI])_{0.9}$ at 30 °C for a) ^{1}H, b) ^{19}F and c) ^{7}Li, where *B* is a prefactor defined by $B = \gamma^2 g^2 \delta^2 \left(\Delta - \frac{\delta}{3}\right)$ where γ is the nuclear gyromagnetic ratio, g is the gradient strength, Δ is the diffusion time and δ is the gradient pulse length. B is shorthand for the Stejskal Tanner equation $S = S_0 e^{-\gamma^2 g^2 \delta^2 (\Delta - \frac{\delta}{3}) D}$ written as: $S = S_0 e^{-BD}$ for measuring the diffusion coefficient where S is the measured NMR signal intensity, S_0 is the measured signal intensity in the absence of diffusion effects (e.g., the signal measured with no field gradients applied).

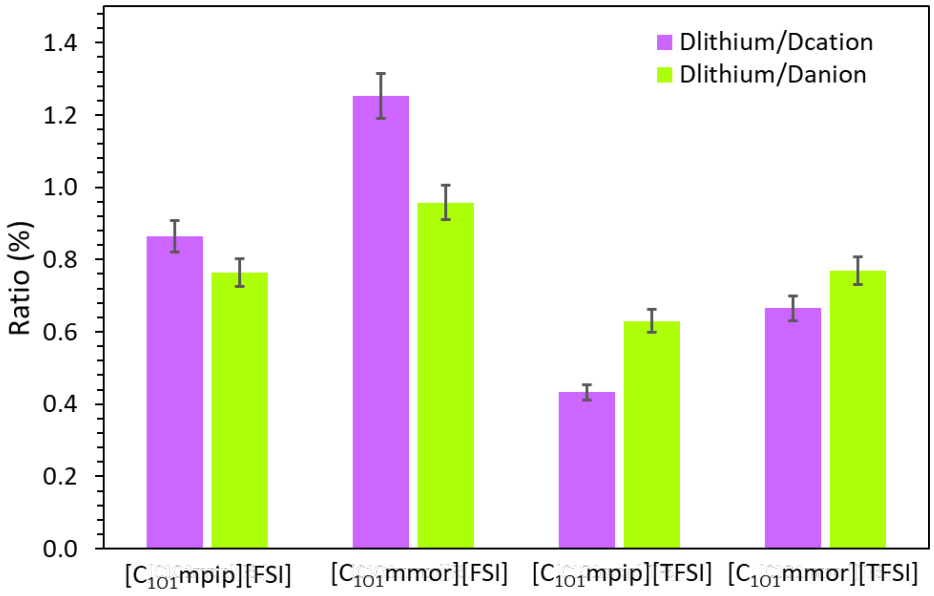

Figure S5. Diffusion coefficient ratios of $D_s(^7Li)$/ $D_s(^1H)$ (purple) and $D_s(^7Li)/D_s(^{19}F)$ (green).

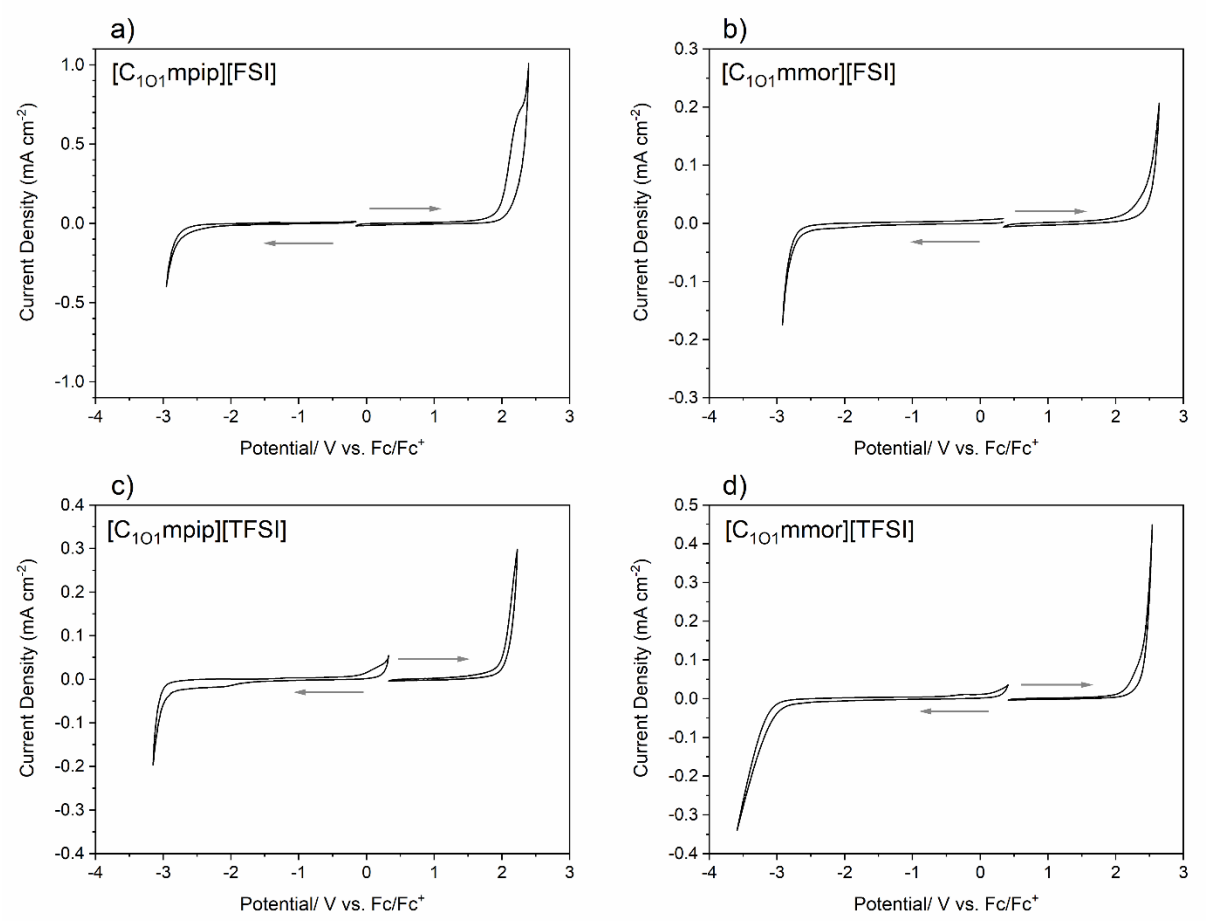

Figure S6. Cyclic Voltammetry of a) $[C_{101}mpip][FSI]$, b) $[C_{101}mmor][FSI]$, c) $[C_{101}mpip][TFSI]$ and d) $[C_{101}mmor][TFSI]$. All experiments were conducted at 25 °C at a scan rate of 20 mV s^{-1}, with a GC working electrode, Pt coil counter electrode and AgOTf reference electrode. Ferrocene was used as an internal reference (Fc/Fc^+ peak E_m $[C_{101}mpip][FSI]$= +0.15 V; E_m $[C_{101}mmor][FSI]$= -0.34 V; E_m $[C_{101}mpip][TFSI]$= -0.33 V; E_m $[C_{101}mmor][TFSI]$= -0.41 V vs. Ag/Ag^+).

Infrared Spectroscopy

The frequency range presented in Figure S2 shows absorbance lines due to the presence of two different anion conformers, *cis*- and *trans*- TFSI. The peaks between 580 and 680 cm^{-1} have been deconvoluted into two peaks with a Gaussian fitting, and estimation of the ratio of the conformers has been obtained. The ratio of the two conformers is described by the Boltzmann factor and can be used to calculate the enthalpy difference between them. The concentration ratio of the conformers is described in Equation S2.

$$r = \frac{I_{600} + I_{650}}{I_{625}} = \frac{[C_{cis}]}{[C_{trans}]} \quad \text{(S2)}$$

Where I_x is the integrated IR intensity of the band at each wavenumber. The equilibrium constant (K) between the two conformers is given in Equation S3 by using the differences in enthalpy (ΔH) and entropy (ΔS). Since r proportional to K, Equation S3 can be transformed into Equation S4.[5]

$$-RTlnK = \Delta H - T\Delta S \quad \text{(S3)}$$

$$\ln(r) = -\frac{1}{T}\cdot\frac{\Delta H}{R} + \frac{\Delta S}{R} + c \quad \text{(S4)}$$

Where c is a constant. Figure S6 reports ln(r) vs. 1000/ T (K^{-1}) of [C_{101}mpip][TFSI] and [C_{101}mmor][TFSI] and their two electrolyte solutions, whereby the slope equals -ΔH/R.

Upon heating, the intensity of the cis-TFSI peak increases, while the peak for trans-TFSI decreases, confirming *trans*-TFSI is the most stable conformer, as reported elsewhere.[6] From the slopes of the linear regression, ΔH = 5.5 kJ mol^{-1} and 6.1 kJ mol^{-1} for [C_{101}mpip][TFSI] and [C_{101}mmor][TFSI] respectively. A higher ΔH indicates that there will be a higher concentration of the more stable, lower energy *trans*-TFSI conformer at a given temperature. The ΔH values were reduced upon lithiation. The piperidinium IL has resulted in a lower enthalpy difference compared to the morpholinium IL, indicating stronger interactions between the cation and anion.

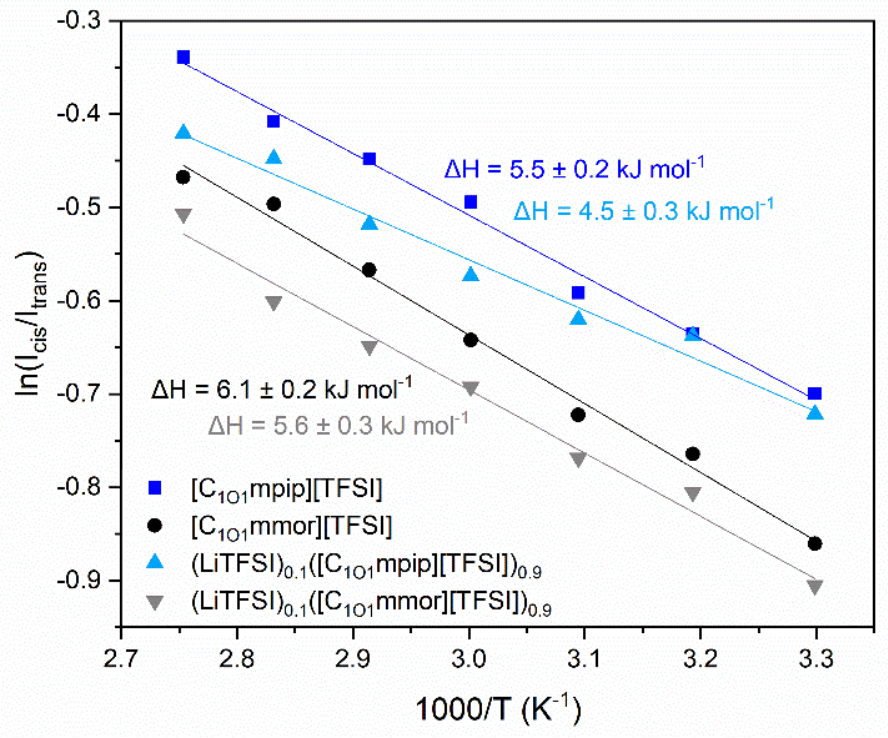

Figure S7. Temperature dependence of the natural logarithm of the ratio of the intensities of the *cis*- and *trans*-TFSI conformer bands with lines of best fit obtained for [C_{101}mpip][TFSI] and [C_{101}mmor][TFSI] and their 10 mol% LiTFSI electrolyte solutions, measured on heating.

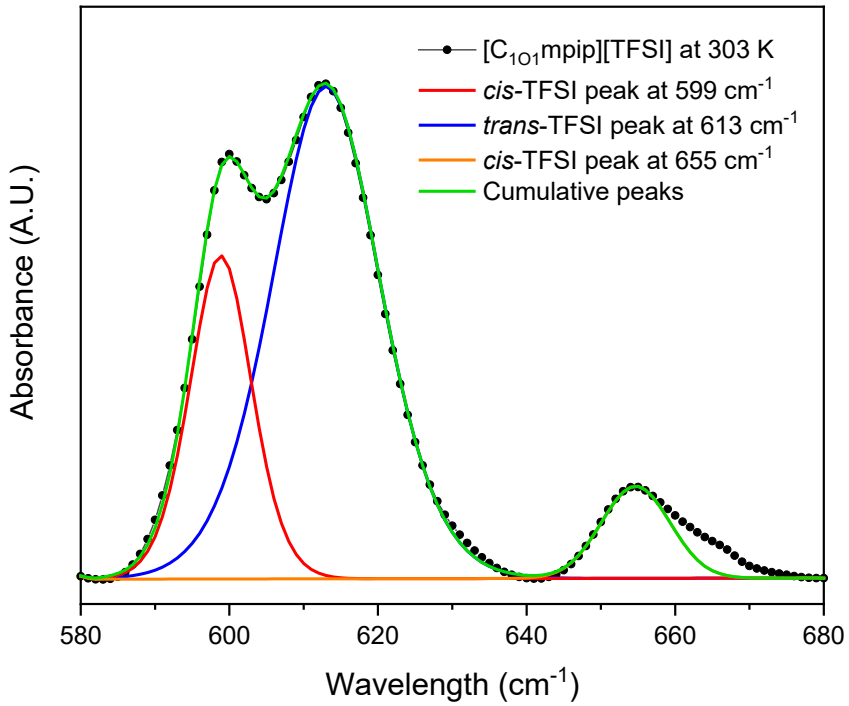

Figure S8. Example of deconvoluted IR spectra of $[C_{1O1}mpip][TFSI]$ at 303 K.

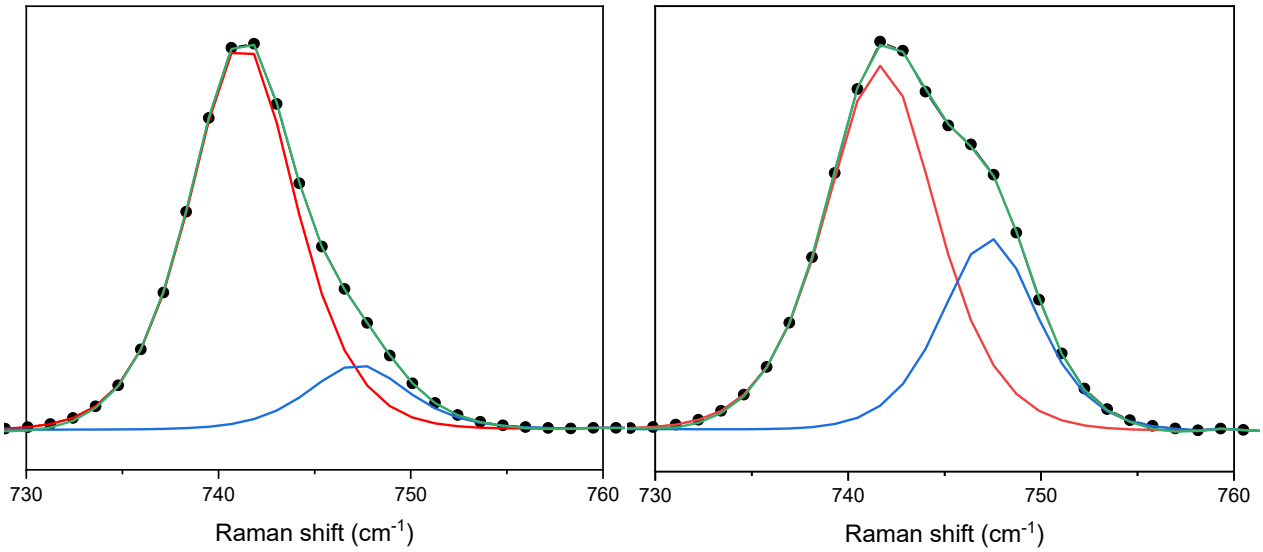

Figure S9. Examples of deconvoluted Raman spectra with $(LiTFSI)_{0.075}([C_{1O1}mmor][TFSI])_{0.925}$ (left) and $(LiTFSI)_{0.2}([C_{1O1}mmor][TFSI])_{0.8}$ (right).

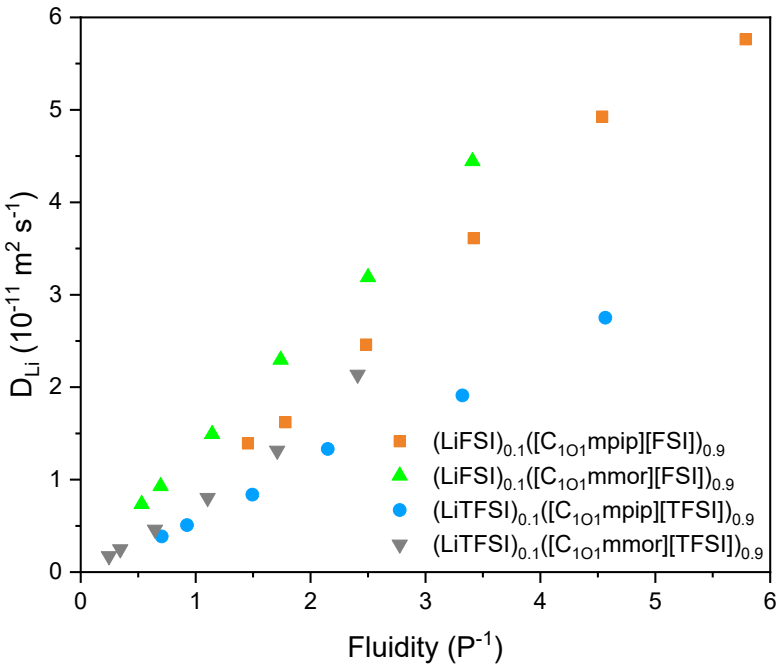

Figure S10. Fluidity (reciprocal viscosity) vs. Lithium diffusion coefficients of each electrolyte system.

References

1 T. Frömling, M. Kunze, M. Schönhoff, J. Sundermeyer and B. Roling, Enhanced lithium transference numbers in ionic liquid electrolytes, *J. Phys. Chem. B*, 2008, **112**, 12985–12990.

2 F. U. Shah, O. I. Gnezdilov, I. A. Khan, A. Filippov, N. A. Slad and P. Johansson, Structural and ion dynamics in fluorine-free oligoether carboxylate ionic liquid-based electrolytes, *J. Phys. Chem. B*, 2020, **124**, 9690–9700.

3 V. L. Martins, N. Sanchez-Ramirez, M. C. C. Ribeiro and R. M. Torresi, Two phosphonium ionic liquids with high Li^+ transport number, *Phys. Chem. Chem. Phys.*, 2015, **17**, 23041–23051.

4 K. Araño, D. Mazouzi, R. Kerr, B. Lestriez, J. Le Bideau, P. C. Howlett, N. Dupré, M. Forsyth and D. Guyomard, Understanding the Superior Cycling Performance of Si Anode in Highly Concentrated Phosphonium-Based Ionic Liquid Electrolyte, *J. Electrochem. Soc.*, 2020, **167**, 120520.

5 F. M. Vitucci, F. Trequattrini, O. Palumbo, J. B. Brubach, P. Roy, M. A. Navarra, S. Panero and A. Paolone, Stabilization of different conformers of bis(trifluoromethanesulfonyl)imide anion in ammonium-based ionic liquids at low temperatures, *J. Phys. Chem. A*, 2014, **118**, 8758–8764.

6 J. C. Lassègues, J. Grondin, C. Aupetit and P. Johansson, Spectroscopic identification of the lithium ion transporting species in LiTFSI-doped ionic liquids, *J. Phys. Chem. A*, 2009, **113**, 305–314.